RGNZ/MGPB

Enhanced desorption of Cobalt from contaminated sandy silty-clay soils

Rudarsko-geološko-naftni zbornik
(The Mining-Geology-Petroleum Engineering Bulletin)
DOI: 10.17794/rgn.2026.3.8

Original scientific paper

Tamás Bacsó[1,2]*, Márton Tóth[1]
[1] *Institute of Water Resources and Environmental Management, University of Miskolc, H-3515 Miskolc, Egyetem str. 1.*
[2] *Adept Enviro Ltd., H-1111 Budapest, Lágymányosi str. 12.*

Abstract
In the present study, we investigated the potential for enhancing the desorption of cobalt contamination in a sandy silty-clay soil contaminated with Cobalt(II)-chloride-hexahydrate. In soils containing silt–clay fractions, effective remediation is primarily prevented by strong surface binding and adsorption processes. Overcoming these limitations requires the establishment of favourable conditions for desorption. In contrast to industrial practices, the potential for desorption was investigated under gradually alkalinizing and reducing conditions. Based on the results, the decrease in the ORP of the saturated system, together with the increase in pH, initiated cobalt desorption. Consequently, within the range above a redox potential from 0 mV to -80 mV and above pH 7.8, the $[Co(H_2O)_6]^{2+}$ cobalt-complex initially formed. Further alkalinization and decreasing redox potential led to the precipitation of the remaining contaminant as $Co(OH)_2$ cobalt hydroxide. As a result of treatment, an average of 7.33 mg of cobalt was desorbed from the silty-clay surface within 29 days from the initiation of the desorption treatment, corresponding to about 12% of the contaminant present in the system. Furthermore, a lognormal distribution-based prediction function series (average R^2 = 0.941) was fitted to the obtained concentration data. The results indicate, that the applied procedure is capable of desorbing approximately 15% of cobalt contaminant, which presumably indicates the desorption capacity of the system. The applied method is widely accessible, cost-effective, and environmentally friendly which qualities that are essential for industrial application. The proposed novel approach represents an efficient and effective complementary technique for the future remediation of certain heavy metal compounds.

Keywords:
remediation, adsorption, desorption, sandy silty-clay soils, cobalt

1. Introduction

Due to intensive industrial activities over the past decades, substantial amounts of toxic heavy metal derivatives have accumulated in subsurface environments. Remediation of these contaminants – particularly in soils with high silt and clay content – remains a major challenge, as it is a costly and complex process for which no widely accepted and effective treatment method currently exists. One of the primary obstacles to successful remediation is the strong adsorption of contaminants onto soil surfaces, which continuously replenishes groundwater pollution through back-diffusion processes. The present study aims to explore strategies for mobilizing cobalt adsorbed onto soil surfaces and to identify conditions that can enhance the extent of its desorption.

The present research focuses on cobalt, an inorganic heavy metal component that, owing to its unique properties, has become an indispensable element in certain modern industrial applications. However, when released into the environment at high concentrations, cobalt is highly toxic to aquatic organisms and poses a significant risk to human health. This study presents the results of a novel remediation approach aimed at enhancing cobalt desorption in soil with high clay mineral content, in sandy silty-clay soil. Our hypothesis is that the combined effect of the alkalinizing compounds added to the assembled column system and the reductive shift of the medium facilitates the transformation of adsorbed cobalt. Initially, this leads to the formation of complex species, which ultimately precipitate from the system. Finally, this section provides an overview of the major soil components, highlighting their key sorption characteristics, and outlines the principal physicochemical properties of cobalt that are relevant to its environmental behaviour.

1.1. Soil properties significant in term of adsorption

The key properties influencing the interactions between soil and any contaminant include soil pH, the nature and quantity of soil colloids, organic matter content,

* Corresponding author: Tamás Bacsó
e-mail address: tamas.bacso@outlook.com
Received: 9 September 2025. Accepted: 4 December 2025.
Available online: 14 May 2026

as well as soil structure and permeability (**Filep et al., 2002**). Additional studies have identified several other critical parameters, such as cation exchange capacity (CEC), redox potential, moisture content, and specific surface area of the soil, all of which collectively affect the potential for removing adsorbed contaminants.

Adsorption, as the phenomenon responsible for contaminant retention, primarily occurs on the surfaces of clay minerals and at the edges of their crystal structures, the latter of which are referred to as active sites. In addition to mineral components, soil constituents within the colloidal size range, such as the humus fraction, Fe–Al–Mn (oxy)hydroxides, and silicate clay minerals, play a particularly important role in determining the soil surface characteristics. Most clay minerals and oxides are present in the colloidal fraction of the soil, which strongly influences its physical and chemical properties. They are critically involved in ion adsorption and ion exchange processes, as well as in the adsorption of organic matter. The environmental significance of the soil organic components of the soil manifests in their sorption capacity and, in the case of heavy metals, their chelation ability (**Ertli, 2005**).

Soil colloids represent the most active and reactive components of the soil, typically falling within the particle size range below 0.002 mm. Colloidal mineral particles, including oxides and clay minerals, together with the humic substances adsorbed onto their surfaces, form the so-called clay–humus complex. Soil colloids possess a high specific surface area and are key determinants of interfacial sorption phenomena. Mineral colloids include clay minerals, iron–manganese and aluminum hydroxides and oxyhydroxides, as well as colloidal-sized mineral fragments (**Schaetzl et al., 2015**).

1.2. Characteristics of Cobalt

Cobalt is chemically less reactive, yet it exhibits moderate solubility in both acidic and alkaline media, typically forming various complex compounds in which it can occur in multiple oxidation states.

Cobalt is widely utilized in industrial applications due to its unique properties. The element plays a critical role in the production of specialized metal alloys, which exhibit exceptional heat resistance and wear resistance. These cobalt-based alloys are highly resistant to elevated temperatures and corrosion, making them ideal for industrial applications under extreme conditions. In recent years, the demand for cobalt has significantly increased, primarily driven by its use in battery manufacturing, particularly as a cathode material in lithium-ion batteries. In aqueous media, cobalt compounds often display a reddish colouration and are commonly employed in inks, paints, and varnishes. Biologically, cobalt is an essential trace element that cannot be synthesized by the human body. However, high concentrations of dissolved cobalt are toxic to aquatic organisms, and certain cobalt compounds are classified as carcinogenic, potentially causing skin cancer and cardiovascular issues in humans. Environmental contamination by cobalt is largely a consequence of mining and industrial usage, posing risks to ecosystems, wildlife, and human health (**URL 1**).

2. Methods

The soil sample used in this study was collected from Aszód, Pest County, Hungary. To assess the desorption potential, it was considered essential to perform a detailed geotechnical characterization of the silty-clay soil. The qualitative analysis of the soil sample was refined through sieving and hydrometer methods, determination of consistency limits, and laser particle size analysis.

Prior to the experiments, the soil sample was appropriately prepared: it was dried in an oven at 105°C until constant mass, then crushed in a hammer mill to a particle size of 2 mm, followed by sieving to obtain a uniform fraction (**Szász and Tóth, 2024**).

Since the soil sample is dominated by silt- and clay-sized particles, a hydrometer analysis was also performed to accurately determine the particle size distribution of the finer fractions (**Lopez et al., 2021**). In addition, soil mechanical analyses and laser (HORIBA LA-950) particle size distribution measurements were also performed. Based on the combined evaluation of these analyses was classified as a clayey-silt soil and some of its key properties are presented in **Table 1**. This sample was homogenized with quartz-sand in order to obtain a deposit with more favourable vertical permeability for the experiments, thereby cutting the sampling time. The applied medium-grained quartz-sand mixed into the clay–silt sample was not examined separately, as due to its physical properties, it participates in the adsorption process only to a negligible extent compared to the silty-clay fraction. However, it should be noted that the soil sample used is very close to the clay-silt or silt-clay boundary.

Table 1. Soil mechanical qualification of sample

Sample ID	Ip (%)	Wp (%)	Qualification
Asz	25.53	17.32	silty-clay

Subsequently, the organic matter content as well as the quantity and type of clay minerals were determined, as these properties play a crucial role in adsorption processes. The mineralogical composition of the soil was determined by X-ray diffraction-XRD analysis (see **Table 2**) which provides a detailed and accurate evaluation of the soil's mineral constituents (**Adams, 2005; Zhou et al., 2018**). The chemical constituents of Asz soil-sample can be found in **Table 3** and **Table 4** (LOI index) by XRF analysis.

5 g portion of the finely ground sample was dried in an oven at 120°C for 2 hours to remove all free water

Table 2. Primary mineralogical constituents of soil-sample

Mineralogical composition (wt%)										
Sample ID	**Quartz**	**Calcite**	**Illite**	**Muscovite**	**Albite**	**Smectite**	**Kaolinite**	**Dolomite**	**Orthoclase**	**Chlorite (II)**
Asz (silty-clay)	43.9	21.4	8.3	7.3	6.0	3.9	3.7	1.8	2.4	1.3

Table 3. Chemical constituents of soil-sample

Sample ID	**SiO_2**	**Al_2O_3**	**MgO**	**CaO**	**Na_2O**	**K_2O**	**Fe_2O_3**
Asz (silty-clay)	46.2	10.1	2.3	18.7	0.4	1.8	3.7
Sample ID	**MnO**	**TiO_2**	**P_2O_5**	**S**	**F**	**LOI**	***TOTAL***
Asz (silty-clay)	0.1	0.6	0.1	0.1	<0.3	15.9	*99.9*

Table 4. LOI (Loss on Ignition) value of Asz soil-sample

Parameter	**Measured value**
LOI (m/m%)	**15.9**
a) Hygroscopic and interlayer water (%)	7
b) Total organic content (%)	3
c) Carbonate decomposition - CO_2 (%)	5.9

present in the soil sample. Elemental calibration was performed under a vacuum of 1.2–1.5 Pa using a RIGAKU Supermini 200 WDXRF spectrometer, equipped with LiF200, PET, and XR25 analyzer crystals. From the dried sample, 1.6–1.8 g was placed into a pre-heated and pre-weighed porcelain boat. The prepared specimen was then heated to 1050°C at a controlled rate of 10°C per minute and maintained at this temperature for 15 minutes.

2.1. Parameters affecting adsorption

Adsorption is influenced by a range of physicochemical and environmental parameters. Redox potential exerts a pronounced effect on pollutant behaviour. Under strongly reducing conditions (Eh<-100 mV), the mobility of specific cations may be substantially constrained, thereby influencing their availability and transport. Time constitutes an additional factor, as extended contact periods typically enhance the extent of adsorption, reflecting the progressive nature of sorption equilibria.

Soil pH is equally critical in regulating adsorption processes. Under acidic conditions, the affinity of soils for cations declines, which can result in increased concentrations of toxic heavy metals and organic hydrocarbon contaminants in the pore moisture. Other soil properties, such as cation exchange capacity (CEC) and soil organic matter (SOM), further modulate sorption behaviour. Although these factors are recognized as influential, their roles are not addressed in detail within the scope of this study.

2.2. Sorption tests

In this study, a hypothetical contamination event was modelled, simulating the infiltration of cobalt pollution into the subsurface through column experiments. The tests were conducted in triplicate, with the inclusion of a control column. The sample holders were cylindrical, made of clear, transparent glass, with identical dimensions and geometry (24/20 mm diameter, 400 mm height). Each column was equipped with a filter stone at the bottom, and sampling was facilitated via a teflon-lined tap.

Following the assembly of the column system, a contaminant stock solution was prepared by dissolving 2.8 g of Cobalt-chloride-hexahydrate ($CoCl_2 \cdot 6H_2O$) in 1000 ml of distilled water. The initial pH of the solution was adjusted to 7.7 at a temperature of 29°C. After assembling the column systems, each sample holder was filled with a thoroughly homogenized mixture of 35 g of silty-clay and 35 g of medium-grained quartz sand. From the prepared contaminant solution, 20 ml was applied to each of the three column samples and saturated using a vacuum pump operating at 0.9 bar. The system was then allowed to stand until adsorption equilibrium was established. In total, approximately 56 mg of dissolved cobalt contaminant was introduced into each column. After every sampling event, 20 ml of distilled water was pumped through the system to flush out any residual, non-adsorbed contaminants within the columns. This procedure ensured that subsequent desorption enhancement was solely attributed to the applied reagents. During the first five days of the experiment, three sampling events confirmed the establishment of adsorption equilibrium. The cobalt concentration in the effluent solution was determined to be 0.0 mg/l for all columns, indicating that the introduced contaminant had been completely retained within the system. Adsorption occurred predominantly on the silty-clay particles, as the relatively large particle size of the quartz sand (0.3–0.63 mm) did not facilitate significant adsorption.

Once the adsorption equilibrium was established, a desorption-enhancing treatment was initiated using a mixture of 30% sodium-bicarbonate, 10% monocalcium-phosphate, and 25% sodium aluminum-sulfate, with the remaining volume comprised of cornstarch-equivalent to household baking powder. The treatment solution was prepared by mixing 2 g of the additive blend with 60

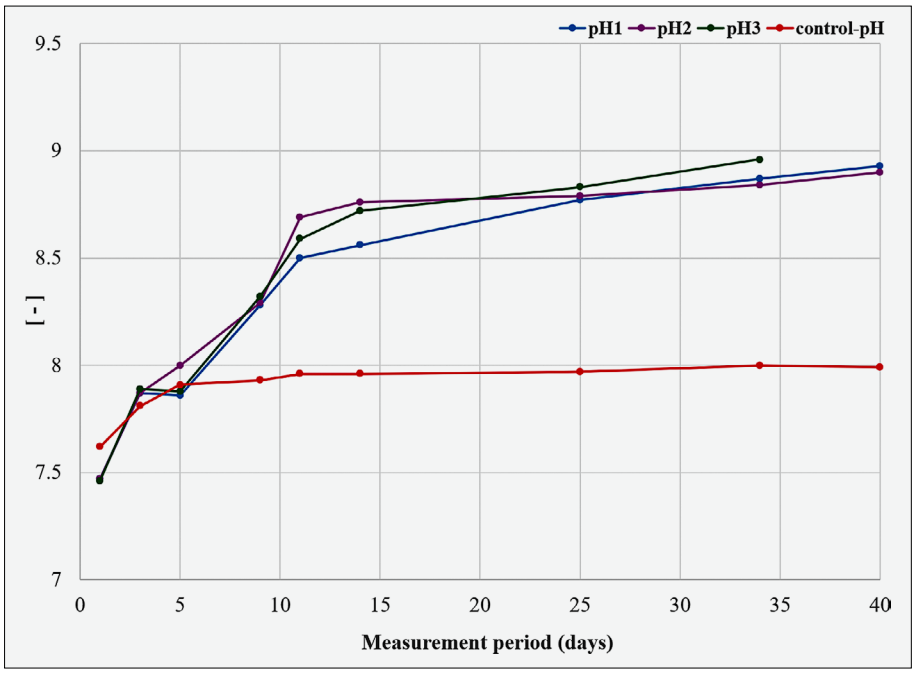

Figure 1. pH-value changes during the whole measurement period

ml of distilled water, which was then applied in equal one-third portions to the three treated columns. The same treatment was administered three times throughout the entire experimental period (on days 5, 8, and 11). In total, 6 g of the dissolved mixture was introduced into the system to enhance cobalt desorption. The initial pH of the treatment solution was pH 8,44. The control column received no treatment, serving as a baseline for the untreated condition. Throughout the experiment, pH, oxidation-reduction potential (ORP), and temperature were continuously monitored to assess temporal changes in the system.

3. Results

To enhance desorption, it was considered essential to shift the established sorption equilibrium toward desorption, which requires modifying the system conditions. It is important to note that, alongside the triplicate column tests, a control column was also included. This control column contained the same amount of soil and cobalt contaminant concentration as the treated columns, labelled Co1–Co3. Thus, the control column appropriately represented the scenario in which the system is left undisturbed, without any external intervention.

Following the initiation of the experimental series, adsorption equilibrium was confirmed in each column by three consecutive measurements over approximately five days. During sampling, the cobalt concentration in the effluent, as well as the pH, oxidation-reduction potential (ORP), and temperature, were continuously recorded as a function of time. The results are illustrated in the series of figures presented below (see **Figures 1–4**).

In **Figure 4**, the cobalt desorption curve is presented as a function of time. Following the complete adsorption of the total cobalt introduced into the system, the desorption-inducing treatment solution was applied, which was added on the 5th day. Based on the measurement results, approximately six days were required for desorption to commence due to the combined effect of the additives and the alkalinization of the medium. Consequently, a gradual increase in cobalt concentration was observed in the effluent samples.

During the desorption phase, an average cobalt concentration of approximately 413 mg/L was determined. It should be noted that, from the onset of desorption, only four sampling events could be performed, as clogging within the columns-caused by the geometry of the applied cylinders-prevented further sampling. As long as effluent samples from the parallel control column consistently exhibited a cobalt concentration of 0.0 mg/L throughout the measurement series following adsorption.

In order to determine the amount of desorbed cobalt contaminant, the obtained concentrations were plotted as a function of the sampling volume, as presented in **Figure 5**.

The amount of desorbed contaminant at the desorption phase points shown in **Figure 5** was determined using the trapezoidal method. The area under the desorption curve was treated as a surface integral, allowing the desorption period to be divided into four segments. The mass of the contaminant within each interval was then calculated according to the following relationship. Assuming f(x) as a continuous function over the interval [a,b], the definite surface integral can be approximated as follows (**Equation 1**):

$$\int_a^b f(x)dx = \frac{a+b}{2}\ dV \qquad (1)$$

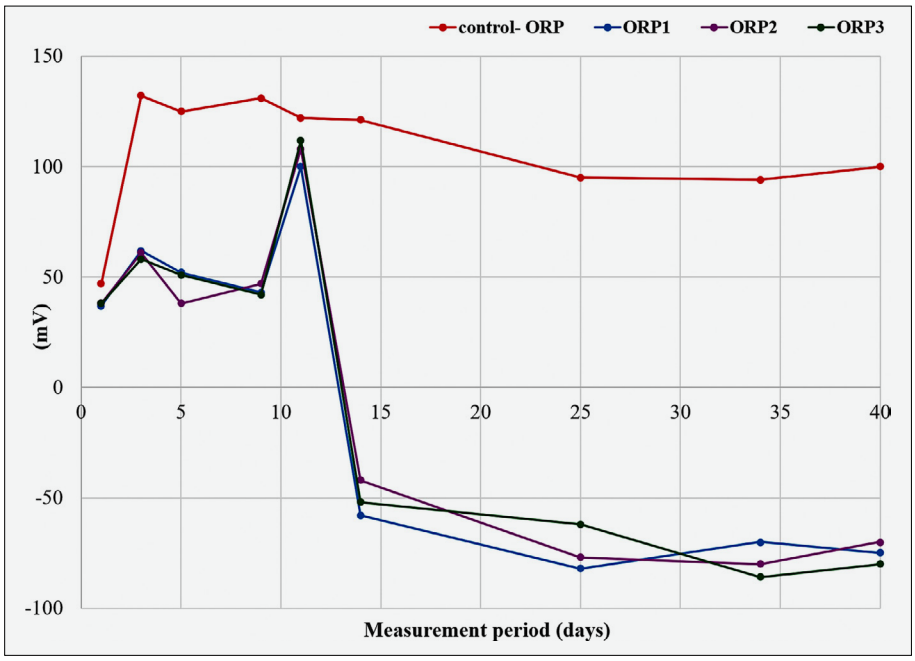

Figure 2. ORP-value changes during the whole measurement period

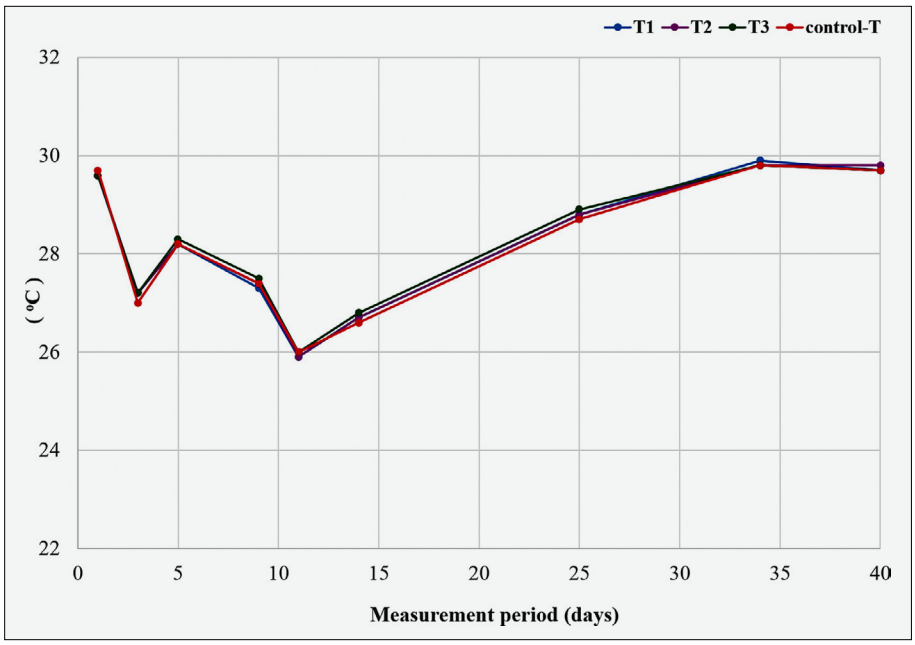

Figure 3. Temperature changes during the whole measurement period

Where:

a – Cobalt concentration of sample-a (mg/dm^3),

b – Cobalt concentration of sample-b (mg/dm^3),

dV – Amount of sampling (cm^3).

In summary, the average concentrations determined during successive sampling periods were multiplied by the corresponding sampling volume, and the resulting values were summed to obtain the area under the curve for the desorption phase, which corresponds to the total mass of cobalt contaminant desorbed from the system. The amount of cobalt released from the system is presented in **Figure 6** and **Table 5**. It must be emphasized, however, that due to colmatation in the sample holders, calculations regarding the initial amount of desorbed contaminant could only be performed based on the first four points of the desorption curve.

The determined cobalt mass at the points of the desorption phase is shown cumulatively in **Table 5**.

4. Discussion

The evaluation of the experimental series begins with the presentation of the measured pH and ORP values, as well as the temperature changes.

The redox potential measured in the treated columns was initially balanced, but during days 11–14 it dropped sharply into the negative range, followed by a further slow yet gradual decline. This trend reflects ongoing bi-

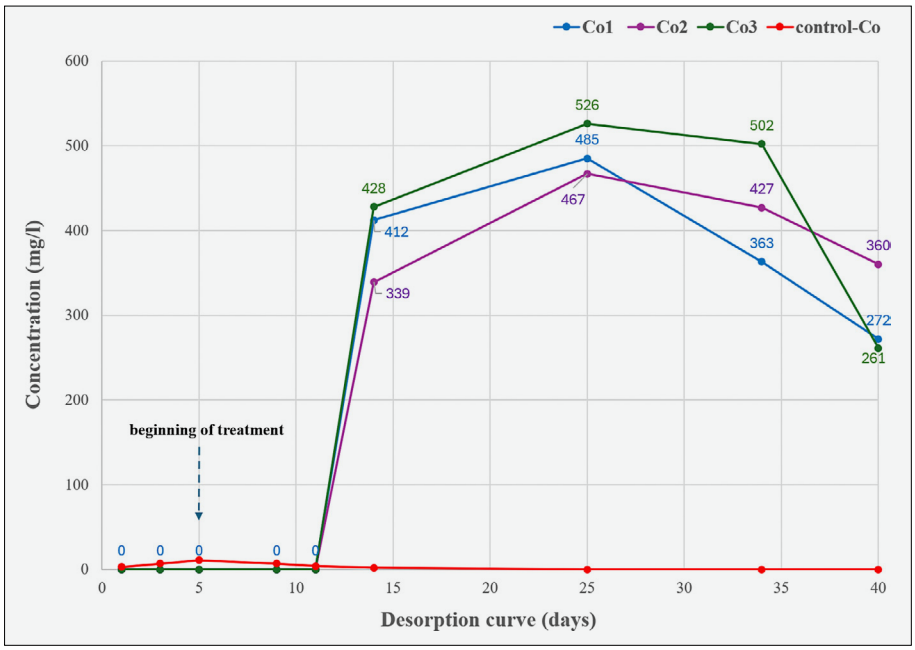

Figure 4. Desorption curve – concentration changes as a result of treatment

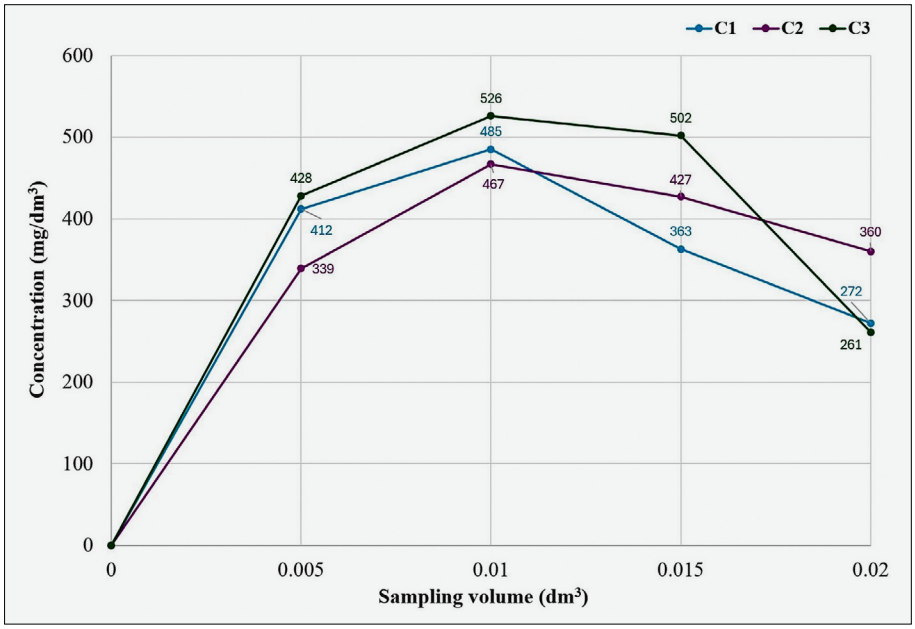

Figure 5. Desorption curve – concentration changes as a function of sampling volume

ological activity within the system, during which bacteria consume dissolved oxygen while degrading the organic matter of the silt–clay matrix. This process led to a decrease in dissolved oxygen concentration, consequently resulting in a reduction of the system's ORP. We have to mention that the addition of phosphate salts can create a reductive environment, leading to anaerobic conditions and a gradual decrease in ORP values. The sodium bicarbonate ($NaHCO_3$) caused a continuous increase in the pH value of water, as higher pH levels render the system less oxidative due to the lower concentration of protons, which contributes to a decrease in redox potential. Finally, the cornstarch present in the treatment solution - which is a simple polysaccharide - has no direct effect on either pH or ORP and is neutral, exhibiting neither acidic or basic properties. However, its potential indirect effect is that soil microorganisms may degrade the starch, resulting in oxidation, which could slightly further decrease the system's ORP.

Furthermore, cobalt compounds exhibit strong affinity for the hydroxyl groups (–OH) present on the surfaces of iron and manganese oxides involving the soil particles. Under the induced reductive conditions, the dissolution of these oxides (Fe^{3+} à Fe^{2+}, Mn^{4+} à Mn^{2+}) releases the cobalt species previously adsorbed or bound to them, thereby enhancing cobalt desorption (**Anthony et al., 2010; Yan et al., 2011; Nicholas, 2013; Clare et al., 1995**).

Moreover, the applied silty–clay soil contains approximately 3% organic matter and under increasingly re-

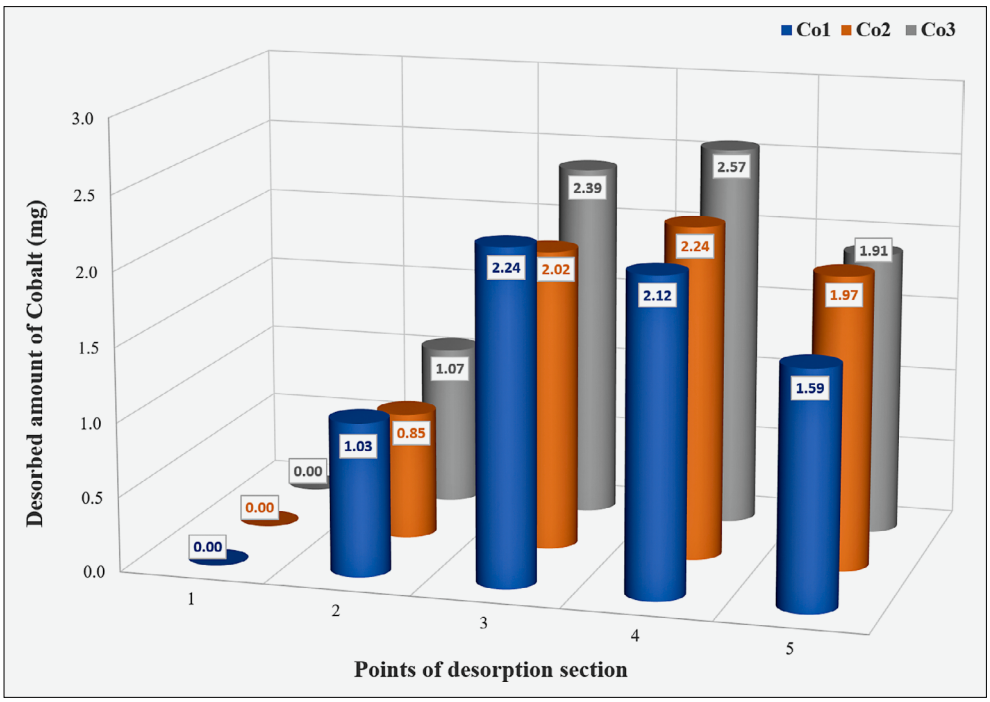

Figure 6. Desorbed amount of cobalt (mg) at desorption section

ductive conditions, the organic colloids lose part of their surface negative charge, which likewise promotes the desorption of bound cobalt.

Continuing with the evaluation of the cobalt concentration curve, it can be observed that following the establishment of sorption equilibrium (effluent cobalt concentration: 0.0 mg/L), we initiated the enhancement of desorption. After treatment of the Co1-Co2-Co3 columns, six days were required for the induced redox potential to start the cobalt desorption process.

We examined the chemical forms of cobalt compounds under the induced pH and redox potential conditions, as illustrated by the Pourbaix diagram. This diagram is one of the most important tools for understanding adsorption and metal ion speciation in water-saturated systems. The combined effect of pH and redox potential determines the redox state of the chemical environment, indicating the types of electron transfer processes occurring within the system. An aqueous solution of Cobalt(II)-chloride-hexahydrate formed the $[Co(H_2O)6]^{2+}$ water complex (Equation 2) under modified medium parameters (decreasing ORP, higher pH) as described by the following interpretation:

$$CoCl_2\ 6H_2O \rightarrow [Co(H_2O)_6]^{2+} + 2Cl^- \qquad (2)$$

The resulting species remains as a dissolved complex ion within this pH range (until 7,5) and ORP: -300 mV. The effluent solution appeared slightly pink and was clear and transparent. As the medium became increasingly alkaline and reductive, and the pH exceeded a value of 7.8, hydroxide ions (OH^-) became available, leading to the precipitation of the remaining undesorbed

Table 5. Desorbed cumulative amount of cobalt (mg)

Sorption tests (mg)		
Co1	**Co2**	**Co3**
6.98	7.07	7.93

Co^{2+} ions as cobalt(II)- hydroxide, according to the following reaction (**Equation 3**):

$$[Co(H_2O)_6]^{2+} + 2OH^- \rightarrow Co(OH)_2 + 6H_2O \qquad (3)$$

The initially precipitated cobalt contaminant exhibited a dark purple tone, which gradually oxidized in the presence of oxygen from the ambient air, turning dark brown as $Co(OH)_3$ formed. Notably, from the second sampling point of the desorption phase (t=25 days) onwards, the effluent appeared turbid with slight sedimentation, further confirming the precipitation process. Thus, cobalt ions remaining in the system above pH 7.8 did not remain in solution but precipitated. This observation is further supported by the fact that the measured cobalt concentrations began to decrease. Although the observed colour change and the decline in cobalt concentrations do not constitute direct evidence of precipitation, but they strongly suggest that such a process has occurred (**Jing et al., 2009; Yanglong et al., 2005; Yang et al., 2011**). Moreover, the ions from dissolved salts alter the structure of water molecules and the hydration case of the dissolved cobalt ions, restricting their mobility. Consequently, sulfate and phosphate ions draw water away from the hydration case of the dissolved species, enhancing electrostatic interactions and reducing solubility. The solubility product of cobalt hydroxide is ex-

tremely low (5.92×10^{-15}), which further supports its precipitation.

The results indicate that under moderately alkaline conditions (pH>7.8), precipitation occurred which is more likely than the previously assumed cation exchange. Cation exchange would require surface-adsorbed Co^{2+} to be replaced by another cation (e.g. Ca^{2+}, Na^{+}), but in alkaline conditions, the concentration of H^{+} is too low to displace Co^{2+} from the soil surface. In summary, the speciation of the cobalt is governed by its dependence on ORP and pH, as characterized using the cobalt Pourbaix diagram (**Ersin et al., 2016; Kamal et al., 2014; Rou-Chen et al., 2020; Chivot et al., 2008**). This diagram illustrates the chemical forms in which cobalt is stable under varying redox potentials and pH conditions in an aqueous environment. Since the pH of the assembled system continuously increased due to the repeated addition of carbonates, the chemical state of cobalt also evolved in response to the rising pH. Initially, shifting toward desorption equilibrium, cobalt remained in a dissolved state, but subsequently precipitated from the system. Moreover, the applied silty-clay exhibits a strongly negative surface charge under alkaline conditions, making it less capable of retaining Co^{2+}. This demonstrates that heavy metal remediation can be effective not only in so in suitably alkaline environments. While metal precipitation has been studied for pharmaceutical industrial wastewater, its application for environmental remediation has not yet been explored.

The addition of carbonates generated OH^{-} ions in the saturated medium, thereby increasing its alkalinity. Heterotrophic catabolic processes produced CO_2 within the system, which induced the formation of carbonic acid. It dissolved the high calcite content of the soil sample, resulting in the release of additional carbonate ions. The combined effect of these processes led to a gradual increase in pH. Due to the intensified treatment, the proportion of carbonate ions in the system shifted, leaving progressively less carbonic acid within the column. Consequently, the escape of CO_2 reduced the amount of carbonic acid formed, shifting the carbonate equilibrium toward CO_3^{2-}, thereby increasing the pH of the soil solution (**Choi et al., 1998**). The following reaction (**Equation 4**) occurs as a result of CO_2 release:

$$2HCO_3^- \rightleftharpoons CO_3^{2-} + CO_2 + H_2O \quad (4)$$

Furthermore, at the beginning of the measurement series, the acidic functional groups of the soil suppressed the increase in soil-solution pH. As the treatment solution was repeatedly added, the soil's buffering capacity eventually became exhausted, allowing the pH of the soil solution to gradually rise, approaching the initial pH of the treatment solution. In other words, the applied alkaline treatment solution displaced the "acidic" cations, leading to the neutralization of protons on the soil particles, which in turn resulted in an increase in the pH of the effluent. To verify the progressively increasing pH values, we performed a calculation to determine the alkalinity of the system, which is presented below.

The molar mass of the applied $NaHCO_3$ is 84.01 g/mol (**URL 2**). In the treatment solution, a total of 0.6 g $NaHCO_3$ was dissolved in 60 mL of distilled water, which was added to the columns in three portions. Consequently, each column received 0.2 g $NaHCO_3$, corresponding to 0.00238 mol. Since the treatment was applied three times, approximately 7.14 mmol $NaHCO_3$ was introduced into each soil sample during the measurement series. The HCO_3^- component can act as an acid (pK_2) by donating a proton or as a base (pK_1) by accepting a proton. The dissociation equilibria of the carbonate ion can be expressed in two steps under standard conditions (**Lewis et al., 1999**) at 25°C, as shown below (**Equation 5):**

$$H_2CO_3 \rightleftharpoons H^+ + HCO_3^- \ (\mathrm{pK_1})$$
$$HCO_3 \rightleftharpoons H^+ + CO_3^{2-} \ (\mathrm{pK_2}) \quad (5)$$

The dissociation constants of the carbonate system (i.e. the acid–base equilibrium constants of carbonic acid) express the extent to which carbonic acid (H_2CO_3) dissociates by proton donation into bicarbonate and carbonate ions in aqueous solution. The first and second dissociation constants are as follows (**Equation 6**):

$$pK_1 = -log_{10} K_1 =$$
$$= 6.35 \rightarrow \mathrm{K_1} = 4{,}3\times10^{-7}\ (\mathrm{mol/dm^3})$$

$$pK_2 = -log_{10} K_2 =$$
$$= 10{,}33 \rightarrow \mathrm{K_2} = 4{,}8\times10^{-11}\ (\mathrm{mol/dm^3}) \quad (6)$$

We investigated the relationship between the system's alkalinity and pH. Alkalinity represents the solution's capacity to neutralize acidic conditions, that is, its basic potential, and is composed of the following ions (**Equation 7**):

$$\text{Alkalinity} = [HCO_3^-] + 2[CO_3^{2-}] + [OH^-] - [H^+] \quad (7)$$

which represent the equilibrium (**Equation 8**) concentrations of the carbonates in the system as a function of pH:

$$[HCO_3^-] = \frac{K_1[CO_2]}{[H^+]} \text{ and } [CO_3^{2-}] = \frac{K_1K_2[CO_2]}{[H^+]^2} \quad (8)$$

By solving the above equations, we obtain that $[H^+] = 1.6\times10^{-9}$ M, which corresponds to a solution pH = $-\log_{10}[H^+] = 8.8$, in agreement with the soil-solution pH values measured during the final stage of the experimental series. Finally, we verified by calculation whether the specified initial pH of the applied treatment solution (pH= 8.44) indeed corresponds to the equilibrium pH of the system. The amount of $NaHCO_3$ in a single application was 0.00238 mol, which considering the total added amount, corresponds to a concentration of 0.119 M,

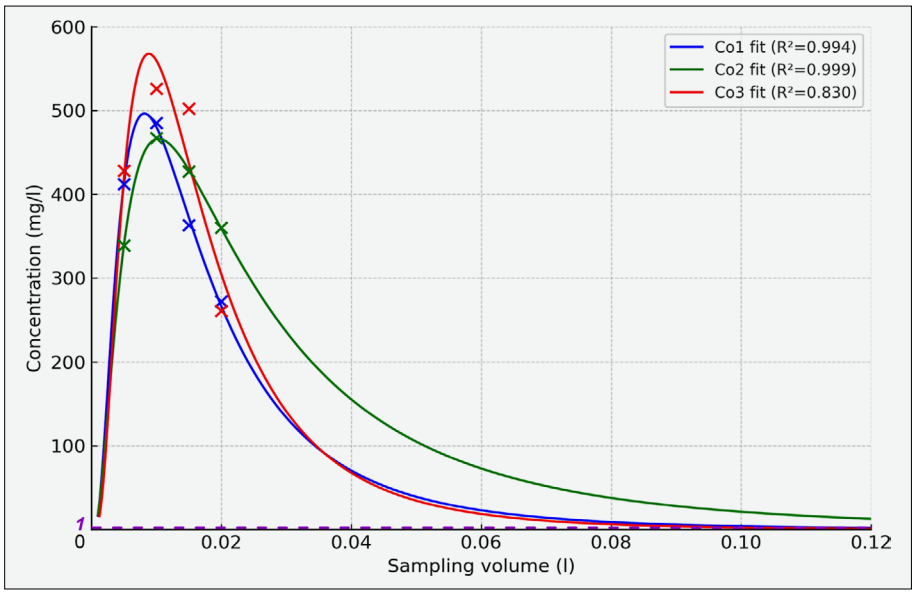

Figure 7. Log-normal fitted function indicating the expected completion of desorption

yielding a calculated pH of 8.34. The discrepancy between the measured and calculated values arises from environmental parameters and the difference of 0.1 is considered as negligible.

During the desorption process, only four samples could be collected, due to column geometry and the resulting colmatation, which prevented further sampling. Based on these data points, we attempted to predict the likely endpoint of desorption by fitting a log-normal function to the desorption curve.

The log-normal distribution is appropriate for modelling the desorption process because it is influenced by multiple factors - binding forces, pore structure, diffusion, pH, ORP - whose combined effect is multiplicative, naturally leading to log-normal behaviour. The binding energy on the soil particle surface is heterogeneous, allowing some contaminant molecules to desorb more readily, while regions with higher binding energy release molecules more slowly. This heterogeneity results in the asymmetric, elongated shape of the desorption curve. Additionally, the desorption rate is not constant; it is initially rapid and gradually slows over time. Consequently, the temporal distribution does not follow a normal distribution but is better described as log-normal.

Thus, the desorption process can be accurately modelled using a log-normal distribution, as illustrated by the predictive curve in **Figure 6**. The log-normal fitting equation (**Equation 9**) was determined according to the method described by **Limpert et al.** (**2001**).

The measured cobalt concentration initially increases slowly, followed by a sharp rise corresponding to the desorption peak concentration, and is subsequently followed by a longer declining phase. The temporal variation of the desorption concentration can be described by the following mathematical relationship, as the process involves the gradual release of the total contaminant load:

$$C(v) = \frac{1}{V\,\sigma\sqrt{2\pi}}\,\exp\left(-\frac{(\ln(V)-\mu)^2}{2\sigma^2}\right) \text{ if V>0;} \quad (9)$$

Where:

- $C(v)$ – concentration as a function of volume (mg/dm^3),
- V – sampling volume (dm^3),
- σ – he standard deviation on the logarithmic time scale (indicates the curve's width),
- μ – the logarithmic mean, which defines the location of the peak of the curve on the log-time scale.

For the modelling of the desorption process, the application of a lognormal function fitting was found to provide an excellent approximation. By solving the mathematical formulation, the efficiency of the desorption process, as well as its potential completion, could be predicted. In **Figure 7**, only the concentration values of the Co1–Co2–Co3 columns were considered to which the lognormal fitting was applied. In accordance with the typical behaviour of a desorption curve, an asymmetric pattern was obtained. The measurement points were initiated from a concentration of 0.0 mg/L, followed by a steeply increasing section where the maximum concentration was reached. This was succeeded by the peak phase, during which the desorption rate attained its maximum, and subsequently by a prolonged, gradually declining section, within which the desorbed cobalt precipitated. A purple dashed-line corresponding to 1.0 mg/L was also indicated on the curve, representing a remediation threshold concentration calculated from an assumed risk assessment.

Based on the lognormal prediction, it was observed that in all three modelled cases the fitted curves showed strong agreement with the measured data. The fitted curves were found to closely follow the experimental values, as demonstrated by R^2 values exceeding 0.99 for

the Co1 and Co2 series and greater than 0.83 for the Co3 series. These results are considered to indicate a very good fit, thereby supporting the applicability of the proposed mathematical model.

With respect to the calculated desorbed mass, it was determined that the amount of cobalt desorbed per column averaged 7.33 mg, which corresponded to approximately 12% of the introduced amount within 29 days. According to the predictive fitting, an additional sampling volume of approximately 0.13 L was required for the Co1 curve, and about 0.1 L for the Co2 and Co3 curves, in order to reach the desorption capacity of the system, i.e. the maximum desorbable amount of contaminant. In summary, when related to the adsorbed cobalt quantity across the Co1, Co2, and Co3 curves, the combined effect of the applied additives was capable of desorbing, on average, a maximum of approximately 15%.

5. Conclusions

To enhance desorption, it is essential to shift the established sorption equilibrium toward desorption by altering environmental conditions and applying newly introduced compounds. The ions of the added salts modified the hydration shell of the dissolved cobalt ions and restricted their mobility, thereby strengthening electrostatic interactions and significantly reducing the water solubility of cobalt. By continuously alkalinizing the column system, desorption was promoted under conditions that have not previously been applied in environmental remediation. Furthermore, cobalt compounds exhibit a strong affinity for the hydroxyl groups located on the surfaces of iron and manganese oxides coating soil particles. Under the induced reductive conditions, the dissolution of these oxides releases the cobalt species previously adsorbed or bound to them, thereby enhancing cobalt desorption. Moreover, as the reducing conditions intensify, organic colloids lose part of their surface negative charge, which likewise promotes the desorption of bound cobalt. In this scenario, the desorbed cobalt contaminant was initially released as a complex species (up to pH 7.8), and with further pH increase (>7.8), it precipitated assumably as cobalt hydroxide.

The predictive analysis of the desorption dataset demonstrated that cobalt desorption was enhanced by the applied novel method, suggesting its applicability as an effective supplementary approach in future remediation technologies. Based on the mass balance calculations of the desorbed contaminant, it was determined that nearly 15% of the introduced cobalt could be removed through this procedure. The additives employed were found to be available in industrial quantities, relatively cheap and effective in the examined soil medium. On the basis of these findings, it can be concluded that the combined application of the precipitation method and the alteration or shift of environmental conditions, such as increasing pH and decreasing ORP, may effectively support future remediation technologies in the case of heavy metals.

Acknowledgement

We would like to express our sincere gratitude to Imre Czinkota, PhD retired Associate Professor at the Institute of Environmental Sciences, Hungarian University of Agriculture and Life Sciences, Gödöllő, for his invaluable professional guidance in the field of chemical sciences, without which this manuscript would not have been possible.

We also extend our thanks to Ádám Bosznai, PhD retired Associate Professor and expert in mathematical modelling at MOHU, for his invaluable professional guidance in the mathematical evaluation of the measurement data series.

6. References

Adams, F. (2005). X-ray absorption and diffraction - Overview. Encyclopedia of Analytical Science, 365–377. https://doi.org/10.1016/b0-12-369397-7/00668-3

Anthony S., William D., Hao Z., John H-T. (2010). The Association of Cobalt with Iron and Manganese (Oxyhydr)oxides in Marine Sediment, Aquatic Geochemistry 16(4):575-585, https://DOI.org/10.1007/s10498-010-9092-1

Chivot, L. Mendoza, C. Mansour, T. Pauporté, M. Cassir (2008). New insight in the behaviour of Co–H2O system at 25–150 °C, based on revised Pourbaix diagrams, Corrosion Science, Volume 50, Issue 1, January 2008, Pages 62-69, https://doi.org/10.1016/j.corsci.2007.07.002

Clare A. B., Ronald G., Andrew W., Roger S. (1995). Kinetics of cadmium and cobalt desorption from iron and manganese oxides; Lincoln University (Pennsylvania), Commonwealth Scientific and Industrial Research Organisation; Soil Science Society of America Journal (Soil Science Society of America)

Lewis, E., Feely, R. A., Millero, F. J. (1999). The optimal carbonate dissociation constants for determining surface water pCO2 from alkalinity and total inorganic carbon, M. Chemistry, Volume 65, Issues 3–4, June 1999, Pages 291-30, https://doi.org/10.1016/S0304-4203(99)00021-3

Ersin,Y., Pelin,A., Oktay,C., Haci,D (2016). Recovery of Cobalt from Sulphate Solutions by Precipitation via Persulphate Oxidation, Conference: 15th International Mineral Processing Symposium (IMPS 2016), Istanbul, Turkey

Ertli, T. (2005). Gyomirtószerek szorpciójának tanulmányozása különböző talaj-oldat rendszerekben. Doktori (PhD) értekezés.

Filep Gy., Kovács B., Lakatos J., Madarász T., Szabó I. (2002). Szennyezett területek kármentesítése, Miskolci Egyetem

Choi, J., Hulseapple, S.M, Conklin, M.H, Harvey, J.W (1998). Modeling CO2 degassing and pH in a stream–aquifer system, Volume 209, Issues 1–4, August 1998, Pages

297-310, Journal of Hydrology, https://doi.org/10.1016/S0022-1694(98)00093-6

Jing Y., Hongwei L., Wayde M., Ray L. F. (2009). Synthesis and Characterization of Cobalt Hydroxide, Cobalt Oxyhydroxide, and Cobalt Oxide Nanodiscs, The Journal of Physical Chemistry.

Kamal R., Célia L., Frédéric G., Myriam D., Chantal G., Jean-Marie H. (2014). Degradation of a cobalt(II)–EDTA complex by photocatalysis and H2O2/UV-C. Application to nuclear wastes containing 60Co, Journal of Radioanalytical and Nuclear Chemistry 303(1):131-137, https://doi.org/10.1007/s10967-014-3311-y

Limpert, E., Stahel, W. A., & Abbt, M. (2001). Log-normal Distributions across the Sciences: Keys and Clues. BioScience, 51(5), 341–352.

Lopez, A., Gustavsson, H., Korkiala-Tanttu, L. (2021). Comparison between hydrometer and laser diffraction methods in the determination of clay content in fine-grained soils, IOP Conf. Series: Earth and Environmental Science 710 (2021) 012012, p.3., https://doi.org/10.1088/1755-1315/710/1/012012

Nicholas C. U. (2013). Cobalt and Manganese, In book., Heavy Metals in Soils (pp.335-366)

Ruo-Chen, X., C. Batchelor-McAuley, E. Rauwel, P. Rauwel, Richard G. (2020). Electrochemical Characterisation of Co@Co(OH)2 Core-Shell Nanoparticles and their Aggregation in Solution, ChemElectroChem. https://doi/10.1002/celc.202001199

Schaetzl, R. J., Thompson, M. L. (2015). "Soils: Genesis and Geomorphology." Cambridge University Press.

Szász N., Tóth A (2025). "Analysis of Atterberg limits of clayey soils exposed to pollutants" Rudarsko-geološko-naftni zbornik, (The Mining-Geology-Petroleum Engineering Bulletin), UDC: 624, https://doi.org/10.17794/rgn.2025.1.8

Zhou, X., Liu, D., Bu, H., Deng, L., Liu, H., Yuan, P., Song, H. (2018). XRD-based quantitative analysis of clay minerals using reference intensity ratios, mineral intensity factors, Rietveld, and full pattern summation methods: A critical review. Solid Earth Sciences, 3(1), 16–29. https://doi: 10.1016/j.sesci.2017.12.002

Yan W., Ren X., Jiu L. (2011): Effect of Fe/Al oxides on desorption of Cd2+ from soils and minerals as related to diffuse layer overlapping Available to Purchase, Research Article, Soil Res (2011) 49 (3): 231–237., https://doi.org/10.1071/SR10148

Yang, J.,Cheng, Hongfei,Frost, Ray L. (2011) Synthesis and characterisation of cobalt hydroxy carbonate $Co_2CO_3(OH)_2$ Nanomaterials. Spectrochimica Acta Part A: Molecular and Biomolecular Spectroscopy, 78(1), pp. 420-428.

Yanglong H., Hiroshi K., Masatsugu S., Toshihiro K., Toshiaki O. (2005). High-Yield Preparation of Uniform Cobalt Hydroxide and Oxide Nanoplatelets and Their Characterization, The Journal of Physical Chemistry B, Vol 109.

URL 1. https://www.ncbi.nlm.nih.gov/books/NBK587403/

URL 2. https://www.chemos.de/import/data/msds/GB_en/144-55-8-A0015267-GB-en.pdf

SAŽETAK

Poboljšana desorpcija kobalta iz onečišćenih pjeskovitih muljevito-glinovitih tala

U ovoj studiji istražena je mogućnost poboljšanja desorpcije kobaltnoga onečišćenja u pjeskovitome, muljevito-glinovitom tlu onečišćenom kobalt(II)-klorid-heksahidratom. U tlima koja sadržavaju frakcije praha i gline učinkovitu sanaciju ponajprije otežavaju jaki procesi površinskoga vezanja i adsorpcije. Prevladavanje tih ograničenja zahtijeva uspostavljanje povoljnih uvjeta za desorpciju. Za razliku od uobičajenih industrijskih praksi, potencijal za desorpciju istražen je pod postupno alkalizirajućim i redukcijskim uvjetima. Na temelju dobivenih rezultata, smanjenje ORP-a zasićenog sustava zajedno s porastom pH potaknulo je desorpciju kobalta. Posljedično, unutar raspona iznad redoks potencijala od 0 mV do –80 mV i iznad pH 7,8, u početku se formirao kobaltov kompleks $[Co(H_2O)_6]^{2+}$. Daljnja alkalizacija i smanjenje redoks potencijala doveli su do taloženja preostale onečišćujuće tvari kao $Co(OH)_2$ kobaltova hidroksida. Kao rezultat tretmana prosječno 7,33 mg kobalta desorbirano je s površine muljevite gline unutar 29 dana od početka tretmana desorpcije, što odgovara oko 12 % onečišćujuće tvari prisutne u sustavu. Nadalje, na temelju dobivenih podataka o koncentraciji prilagođen je niz prediktivnih funkcija temeljen na lognormalnoj raspodjeli (prosječni R^2 = 0,941). Rezultati pokazuju da je primijenjeni postupak sposoban desorbirati približno 15 % kobaltnoga onečišćenja, što vjerojatno upućuje na desorpcijski kapacitet sustava. Primijenjena metoda široko je dostupna, isplativa i ekološki prihvatljiva, što su kvalitete ključne za industrijsku primjenu. Predloženi pristup predstavlja učinkovitu i djelotvornu komplementarnu tehniku za buduću sanaciju određenih spojeva teških metala.

Ključne riječi:
remedijacija, adsorpcija, desorpcija, pjeskovita muljevito-glinovita tla, kobalt

Author's contribution

Tamás Bacsó (PhD student) provided the raw materials preparation, performed the laboratory work and the presentation of the results. **Márton Tóth** (Associate professor) provided the evaluation of the experimental results and the presentation of the results.
All authors have read and agreed to the published version of the manuscript.